

Preliminary Seismic Risk Analysis of a Data Network

Simona Esposito

Swiss Re Management Ltd., Mythenquai 50/60, 8033 Zurich, Switzerland. E-mail: simona_esposito@swissre.com

Alessio Botta

Dipartimento di Ingegneria Elettrica e delle Tecnologie dell'Informazione, Università degli Studi di Napoli Federico II, via Claudio 21, 80125, Naples, Italy. E-mail: alessio.botta@unina.it

Melania De Falco

Dipartimento di Ingegneria Civile, Edile e Ambientale, Università degli Studi di Napoli Federico II, via Claudio 21, 80125, Naples, Italy. E-mail: melania.defalco@unina.it

Adriana Pacifico

Dipartimento di Strutture per l'Ingegneria e l'Architettura, Università degli Studi di Napoli Federico II, via Claudio 21, 80125, Naples, Italy. E-mail: adriana.pacifico@unina.it

Eugenio Chioccarelli

Dipartimento di Ingegneria Civile, dell'Energia, dell'Ambiente e dei Materiali, Università Mediterranea di Reggio Calabria, via Graziella, Reggio Calabria, Italy. E-mail: eugenio.chioccarelli@unirc.it

Antonio Pescapè

Dipartimento di Ingegneria Elettrica e delle Tecnologie dell'Informazione, Università degli Studi di Napoli Federico II, via Claudio 21, 80125, Naples, Italy. E-mail: antonio.pescapè@unina.it

Antonio Santo

Dipartimento di Ingegneria Civile, Edile e Ambientale, Università degli Studi di Napoli Federico II, via Claudio 21, 80125, Naples, Italy. E-mail: antonio.santo@unina.it

Iunio Iervolino

Dipartimento di Strutture per l'Ingegneria e l'Architettura, Università degli Studi di Napoli Federico II, via Claudio 21, 80125, Naples, Italy. E-mail: iunio.iervolino@unina.it

The seismic risk assessment of spatially distributed infrastructures is gaining increasing research attention. Data communication networks, although less investigated than other infrastructures, have large importance for the immediate post-event emergency management and community resilience. In this study the framework of simulation-based probabilistic seismic risk analysis of data communication infrastructures is applied to a real case study; i.e., the interuniversity data network of the Campania region (southern Italy). The network is constituted by point-like facilities, that is, racks located within buildings and containing the devices routing and managing traffic, and distributed links, that is, buried fiber-optic cables. The network performance was assessed following the performance-based earthquake engineering framework extended to spatially distributed systems. The seismological, geological and geotechnical features of the region were characterized together with the seismic vulnerability of each element of the network. Moreover, to overcome the absence of available fragilities for buried fiber-optic cables, and as a difference with respect to previous work of the authors on the topic, the fragilities recently developed for buried electrical cables are adapted. The network performance is quantified in terms of traffic lost, that is the difference between traffic transferred through the network before and after the seismic event. Results indicate a relatively low level of losses when the network's region is hit by an earthquake and, according to the adopted models, a low influence of cables fragility on the performance of the network.

Keywords: civil infrastructure system, performance-based earthquake engineering, failure recovery mechanisms, traffic lost, regional seismic hazard, fragility functions, seismic losses.

1. Introduction

Risk assessment of distribution systems, as gas or transportation networks, is the focus of a significant deal of research in earthquake engineering. This is mainly because the community resilience, intended as the set of

attributes that allows the continuity and/or the restoration of the lifeline and business after a disrupting earthquake event, is also dependent on the seismic performance of the civil infrastructure.

Proceedings of the 30th European Safety and Reliability Conference and the 15th Probabilistic Safety Assessment and Management Conference

Edited by Piero Baraldi, Francesco Di Maio and Enrico Zio

Copyright © ESREL2020-PSAM15 Organizers. Published by Research Publishing, Singapore.

ISBN/DOI: 978-981-14-8593-0

Also electrical and telecommunication networks, in the context of utility systems are important. Components of these networks are cables, either buried and/or running on aerial lines, as well as a number of points of presence (POPs) containing the devices routing and managing traffic. Consequently, in the risk assessment of this kind of systems, these two different typologies of elements should be considered. However, Chang and Wu (2011) and Cavalieri et al. (2014) evaluated the seismic risk of electrical distribution networks accounting for the seismic vulnerabilities of the POPs and neglecting those related to cables: the former analyzes a simplified seismic scenario in which only substation fragilities are considered (according to Vanzi, 1996), while the latter discusses that, being the lines of the analyzed case study aerial lines, they can be considered not seismically vulnerable. On the other hand, Esposito et al. (2018) discuss the seismic performance of an existing data communication network, located in southern Italy (*Rete di Interconnessione Multiservizio Interuniversitaria Campana*, RIMIC). The paper identifies the absence of fragility models for buried fiber-optic cables as a main limitation of results.

In the study herein presented, the seismic risk assessment of the RIMIC is reconsidered adapting the fragility models for electrical buried cables of Kongar et al. (2017) to the case of buried fiber-optic cables. The paper is structured such that main characteristics of a data communication networks, together with the failure recovery mechanism, are presented first. Then, the elements required to extend the performance-based earthquake engineering, or PBEE, to spatially distributed system are summarized. Thus, the analyzed data network is described and the models for simulation of the seismic hazard and the network vulnerability are described. Finally, the preliminary results of the analyses are presented and discussed.

2. Data Communication Networks

A data communication network provides connectivity between individual networks (i.e., telecommunication companies, multiple service providers and end nodes) at various levels through a complex and hierarchical interconnection of nodes and links. Computers at the border of the network (also called end hosts; i.e., devices used by human beings, servers, etc.) are connected through a series of intermediate devices (mainly switches and routers) that manage the traffic. From a physical point of view, the typical structure of a communication network is made of a number of point-like facilities (i.e., the intermediate devices) and distributed links

(mainly fiber optics or copper cables) either buried and/or running on aerial lines.

The intermediate devices usually reside inside the POPs which are located in building facilities that provide appropriate services (electricity, air conditioning, alarm systems, fire protection, etc.) to ensure continuous operation of the devices and the proper installation of suitable racks to house such devices. Each rack contains optical adds/drop multiplexer, switches, routers, and, in general, all the devices needed to handle the traffic of the end users.

Large networks are often organized in a hierarchy, where the highest level forms a backbone for the other levels. Generally, at least two cables connect each POP to other two POPs of the same level. This is to ensure that all the POPs have different paths available, which is an important redundancy requirement, especially for the main loops.

The information exchanged between the end-hosts (e.g., a web page, an image, or a voice flow) is fragmented in a number of pieces called packets that are then transmitted through the network using a simple protocol to exchange data; i.e., the IP (internet protocol). All the packets constitute the so-called network traffic.

2.1 Functionality Failure and Recovery

A key feature of data distribution networks are failure-recovery mechanisms. They are generally implemented by intermediate devices and can be of two main classes, depending on the layer of the protocol stack they operate at: IP-layer and physical-layer.

IP-layer mechanisms (also called routing-layer mechanisms), are realized by routing-algorithms performed by the intermediate devices (the routers in particular). These devices, in case of link and node failures, may be able to automatically find a new path towards the destination through a process called re-routing. The *IP-layer mechanism* requires some time (in the order of minutes) to reach a new configuration and to deliver previously lost packet.

Physical-layer mechanisms operate differently. In case two or more links (e.g., more optical fibers from within the same cable) connect the same two physical layer devices, and one link (the primary) breaks, another one can automatically be used by such devices without being noticed by and/or informing all the other devices. These mechanisms require a shorter time with respect to the previous ones; however, they can be of help only if a part of, but not all, the cables connecting the devices experiencing the failure is broken.

3. Performance-Based Seismic Risk Analysis

3.1 Seismic Hazard

A data communication network is a system made of different components regionally-distributed. This means that the seismic hazard of the region where the network is located has to be evaluated jointly for all the locations of the system's components (e.g., Weatherill et al. 2014). The probabilistic seismic input representation has also to account for the so-called *cross-correlation* (e.g., Loth and Baker 2013) among the ground motion intensity measures (IMs) that are needed for the vulnerability analysis of the different components of the network. In other words, the stochastic dependence between different IMs in each earthquake has to be considered. This last aspect represents the key difference with respect to seismic risk analysis of point-like facilities: the seismic hazard has to be represented in terms of random fields accounting for the statistical dependencies between different ground motion parameters.

Indeed, the network is vulnerable to either ground shaking (transient ground deformation or shaking, *TGD*), that could typically damage POPs, or ground failure (i.e., geotechnical effects resulting in permanent ground deformation, *PGD*) that mainly causes damage to the buried components of the network. Accounting for *PGD* requires the characterization of the susceptibility of the region to landslides and liquefaction. Among the different approaches proposed in literature to model these seismic-induced hazards, the simple approach of HAZUS (FEMA, 2004), represents a base-level scale-compatible application of geotechnical hazard characterization in the context of risk analysis of spatially distributed systems, since it requires limited information about the geotechnical characterization of the region.

3.2 Seismic Vulnerability

To evaluate seismic damage of each component of a distributed network given ground shaking, IMs have to be related to effects by means of models; e.g., fragility functions. For point-like systems (POPs, in this case) these relations typically provide the probability of reaching or exceeding some damage state (DS) given IM. The vulnerability characterization of POPs may be performed analyzing the seismic behavior of the hosting building and their sub-components, in order to identify those critical with respect to seismic fragility.

For buried elements, the fragility models usually consist of a seismic-intensity-dependent rates, providing the average number of damages (e.g., leaks or breaks) per unit-length. Damages

observed in past seismic events shows that buried cables are mostly sensitive to permanent ground deformation induced by liquefaction, landslide and co-seismic rupture (see section 5.2).

3.4 Systemic Performance and Risk

Performance evaluation of infrastructure systems reflects their spatially distributed and functionally interconnected nature, which needs specific indicators (Cavalieri et al., 2014; Franchin and Cavalieri, 2013; Esposito et al., 2015). The identification and description of the relation/interactions between the components of each system (intra-dependencies) and inter-relations between the systems (inter-dependencies) is a fundamental step for the evaluation of the state of the system (i.e., the performance) as a function of the states of its components and of other systems. The quantitative measure of the performance of the whole system and its elements is usually given by performance indicators (PI's).

One possible PI is the traffic flowing through the network. It is used in this paper to evaluate the seismic performance of the network comparing the amount of traffic before and after the seismic event. In fact, in this work a *capacity* analysis is performed; this type of analysis allows to estimate capacitive flows of the network, based on the damages sustained by the network components. The amount of traffic is dependent both on the number and kind of users and on the capacity of the network to actually transport such traffic to its intended destination. Therefore, the *traffic matrix* of the network has to be considered. Such a matrix basically contains the volume of traffic exchanged by any two nodes in the network. It is assumed that after an earthquake event, any two nodes can still be able to exchange traffic, if at least one path connecting them is still available.

4. The RIMIC data network

4.1 Network Description

The studied network is an infrastructure deployed in the Campania Region of Italy as part of a publicly financed project called *Rete di Interconnessione Multiservizio Interuniversitaria Campana*, RIMIC. The project has created a high-speed and high-redundancy network connecting the universities, research centers, and public institutions of the region. Physically, the network is configured as a ring system: the first ring (or loop) has regional coverage and additional rings are connected to it for covering the Metropolitan Area Networks; the latter are the provinces of Naples (NA), Caserta (CE), Benevento (BN), and Salerno (SA). RIMIC has several sub-networks, however only the main loop (Fig. 1) is considered

in this study (for a more detailed description of the network see Esposito et al., 2018).

The four network POPs are located in university buildings, one for each province covered by the network, and are connected by a ring of about 280 km of optical fibers. The main characteristics of the buildings and the corresponding vulnerability class according to HAZUS (FEMA, 2004) taxonomy are summarized section 5.2.

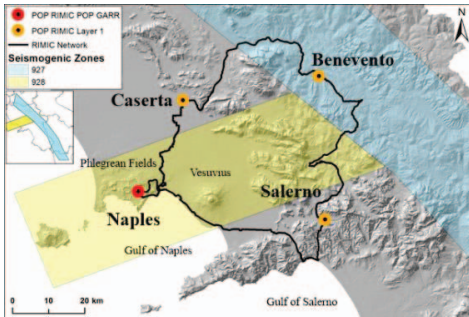


Fig. 1. The main loop of the RIMIC network and the location of POPs. The two seismogenic zones considered in the analyses are also represented (see also section 5.1).

The fiber optics links are mainly housed along roads, railroads and in some parts along bridges decking systems and tunnels. Fiber optic cable lines are buried at about 1 m and have a diameter of 50 mm. They are made of a central strength member that provide the rigidity to keep the cable from buckling and protect the individual fiber optical cables from breaking during the installation.

In the analysis presented herein, the network is considered able to instantaneously reroute traffic on the available links or paths.

4.2 Seismotectonic and Geological Setting

The network is mainly affected by two seismic source zones; i.e., those named as 927 and 928 according to the seismic source model of Meletti et al. (2008). (Data characterizing the two seismic zones are given in section 5.1.)

RIMIC lies on different geological formations (see Esposito et al., 2018), mainly located in plains and riverine contexts and only in few cases along slopes. The shallower layers (2-3 m depth) are constituted by pyroclastic materials, debris, paleosols and infillings, but available information are not sufficient to account for them and only the geological bedrock was considered in the analyses. Similarly, cables may be located along concrete structures (tunnels and bridges) but their existence was also neglected.

5. Analysis

The network performance was assessed evaluating the amount of traffic that is correctly transferred through the network to the POPs, considering the traffic demand change after an earthquake. Both *TGD* and *PGD* hazards were accounted for. Fiber cables and POPs were considered the vulnerable elements, and the risk assessment was performed in terms of the described PI.

The simulation was performed using the object-oriented framework for infrastructure modeling and simulation (OOFIMS, <https://sites.google.com/a/uniroma1.it/oofims/>) software (Franchin and Cavalieri, 2013) for the seismic risk assessment of interconnected infrastructural systems.

5.1. Simulation of Seismic Input

Following the methodology proposed in Esposito et al. (2015) and considering all the aspects discussed in section 3, the network assessment was performed via Monte Carlo simulations. In each simulation, the seismic event is simulated in terms of earthquake location and magnitude considering the two discussed seismic sources. The magnitude of each event is computed considering an exponential truncated Gutenberg-Richter distribution (Gutenberg and Richter, 1944) characterized by minimum and maximum (surface wave) magnitude values (M_{min} and M_{max} respectively), the annual rate of earthquake occurrence above M_{min} , ν , and the negative slope of the Gutenberg–Richter relation, b . These data are taken from Barani et al. (2009) and are summarized in Table 1. Given the magnitude, the simulation of the earthquake on the two seismic zones was in terms of location, which was assumed as uniformly distributed over each source zone.

Table 1. Parameters of the selected seismic source zones.

Zone	ν (1/year)	b	M_{min}	M_{max}	Prevalent fault mechanism
927	0.362	0.557	4.3	7.3	normal
928	0.054	1.056	4.3	5.8	normal

The earthquake IM considered in the analysis is the *peak ground acceleration* or *PGA*, to be consistent with fragility curves used for the vulnerability analysis (see next section). Considering the ground motion prediction equation (GMPE) by Bommer et al. (2012), Eq. (1), the *PGA* value at the bedrock of a generic site, say j , produced by the earthquake of given magnitude and distance generated in the i -th simulation, is evaluated as:

$$\log(PGA_{i,j}) = E(\log(PGA) | m_i, r_{i,j}, \theta) + \eta_i + \varepsilon_{i,j} \quad (1)$$

In the equation, $PGA_{i,j}$ denotes the PGA at the site j due to earthquake i ; $E(\log(PGA)|m_i, r_{i,j}, \theta)$ is the expected value of its logarithm, conditional to the earthquake of known magnitude (m_i), source-to-site distance ($r_{i,j}$) and rupture mechanism (θ); η_j is the inter-event residual, common to all sites, and assumed as a normally distributed random variable with zero mean and standard deviation σ_{inter} (from the GMPE model); $\varepsilon_{i,j}$ is the intra-event (site-to-site in the same event) heterogeneity of ground motion, usually modeled via a multivariate zero-mean Gaussian distribution with covariance matrix reflecting correlation as a function of inter-site distance (see Jayaram and Baker, 2009). (In this case, the intra-event residual model formulated by Esposito and Iervolino (2011) for PGA was used.)

The average shear-wave velocity between 0 m and 30 m depth, were considered to account for local site conditions (Forte et al., 2017) and to transform the PGA at the bedrock in the PGA at the surface, PGA_s , adopting the soil coefficients of Bommer et al. (2012).

As it regards landsliding hazard, according to the HAZUS (FEMA, 2004) procedure, a landslide susceptibility map was obtained based on the geological groups, slope angles, and groundwater conditions of the study area. This map was finally transformed into the critical acceleration (k_c) map shown in Fig. 2a, adopting the simplified method by Wilson and Keefer (1985). According to this approach, in each simulated earthquake, permanent displacements occur or not in a susceptible deposit, in those cases in which the PGA at the surface, PGA_s , exceeds k_c . The mean of the resulting displacement induced by landslide (PGD_{land}) is calculated via the Saygili and Rathje (2008) empirical model; Eq. (2). The model has a residual with a standard deviation $\sigma_{\ln(PGD_{land})}$.

$$\ln(PGD_{land}) = 5.52 - 4.43 \cdot \left(\frac{k_c}{PGA_s}\right) - 20.39 \cdot \left(\frac{k_c}{PGA_s}\right)^2 + 42.61 \cdot \left(\frac{k_c}{PGA_s}\right)^3 - 28.74 \cdot \left(\frac{k_c}{PGA_s}\right)^4 + 0.72 \cdot \ln(PGA_s) \quad (2)$$

A liquefaction susceptibility degree was also assigned (none, moderate, high, and very high) according to the HAZUS procedure, to obtain the liquefaction potential map (Fig. 2b). Each liquefaction susceptibility category (SC) has associated site specific liquefaction coefficients, given in the HAZUS manual and derived, from the empirical models of Liao et al. (1988), as well as correction factors that depends on the groundwater depths and the magnitude of the event (see Seed and Idriss, 1982 for more details).

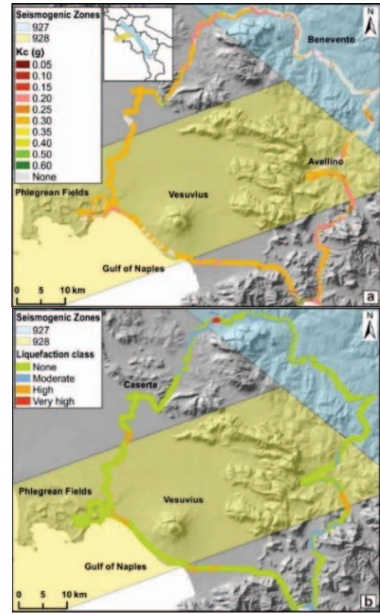


Fig. 2. (a) k_c Critical acceleration map; (b) liquefaction susceptibility map.

The likelihood that an earthquake will be able to initiate the phenomenon is then evaluated for each SC as a function of these site-specific coefficients and correction factors.

Given that liquefaction occurs, the displacement due to lateral spreading (PGD_{LS}) and the displacement due to settlement (PGD_{SET}) can be estimated. PGD_{LS} is evaluated (in meters) following Eq. (3):

$$PGD_{LS} = 0.0254 \cdot K_{\Delta} \cdot PGD \quad (3)$$

where PGD is the expected displacement for each susceptibility category under the normalized level of shaking and K_{Δ} is a displacement correction term calculated from Seed and Idriss (1982). While, PGD_{SET} is a characteristic settlement attributed to each susceptibility class (FEMA, 2004) determined via the approach by Tokimatsu and Seed (1987).

5.2. Damage Assessment

To evaluate the earthquake-induced damage in each simulation, IMs were related to system component damage via fragility models. In this case, the functionality of the nodes depends on the seismic behavior of the building housing and on the response of the non-structural component; i.e., the rack. In particular, the complete loss of functionality of each POP (complete damage state; i.e., no data transmission) has been attributed to the building collapse (complete damage state) or sliding or overturning of the rack resulting in malfunction. The vulnerability of the

rack has been characterized through the use of the fragility curves for acceleration-sensitive non-structural components developed by HAZUS (FEMA, 2004). In particular, the sliding or overturning of the rack corresponds to moderate damage state of the fragility curves developed by HAZUS. To this aim, the building typology, height and the seismic code of the four buildings was identified according to the HAZUS taxonomy and the corresponding vulnerability class was associated as summarized in Table 2.

Table 2. HAZUS (FEMA, 2004) class for the vulnerability characterization of the non-structural components (racks).

	Naples	Salerno	Benevento	Caserta
Building typology	Reinforced Concrete (RC)	RC	Unreinforced Masonry (URM)	RC with URM walls
Floors	3	1	3	3
Seismic code	Moderate Code	Moderate Code	Pre-Code	Low Code
HAZUS Class (Rack)	C2L	C1L	URMM	C3L

The vulnerability of the building has been characterized through the use of lognormal fragility functions available in literature selected using the FRAME software (Petruzzelli and Iervolino, 2014) according to the structural typology, material, height and seismic code level. Median and standard deviation of the logarithm, β , of the selected fragility functions and the selected references are summarized in Table 3.

Table 3. Fragility functions selected for the building housing of each node of the network.

	Naples	Salerno	Benevento	Caserta
IM	<i>PGA</i>	<i>PGA</i>	<i>PGA</i>	<i>PGA</i>
DS	Complete	Complete	DS5	DS5
Median [g]	0.78	0.78	0.41	7.31
β	0.33	0.33	0.73	2.00
Reference	Tsionis et al. (2011)	Tsionis et al. (2011)	Kappos et al. (2003)	Rota et al. (2008)

Regarding the optical fiber cables, there are no suitable fragility functions available in literature and in Esposito et al. (2018) a simplified expert-based model was adopted. However, Kongar et al. (2017) analyzed the seismic performance of buried electrical cables of medium voltage network collecting the observed damages caused by the 2010–2011 Canterbury seismic sequence in New Zealand. Here the fragility models of Kongar et al. (2017) are adopted for the fiber optic cables of the network.

According to the cited paper, *TGD* has negligible effects on cables while the repair rate

(RR) of cables subjected to soil liquefaction is expressed by Eq. (4) in which PGD_{liq} is equal to the geometric mean of PGD_{LS} and PGD_{SET} , whereas α is a coefficient that depends on the insulation material. In particular, $\alpha = 0.26$ is associated to cables insulated by cross-linked polyethylene, that are the less vulnerable among those analyzed, whereas the most vulnerable typology is represented by $\alpha = 1.07$. In the following, shown results are obtained with both values of α to discuss its influence on the network performance.

$$RR = \alpha \cdot (4.317 \cdot PGD_{liq} - 0.324) \quad (4)$$

As pertaining to landslide, no equivalent relations between PGD_{land} and RR are known. Thus, it is here assumed that when the site is interested by landslide, Eq. (4) can be applied substituting PGD_{liq} with PGD_{land} .

5.3. Performance and risk assessment

The seismic performance of the network has been carried out in each run via a capacity analysis, evaluating the total traffic delivered to each destination before and after the seismic event. To this aim, the network (considered bi-directional) has been modeled as a graph characterized by a connectivity matrix (Fig. 3 on the left); an example of traffic matrix for a particular hour of the day is shown in Fig. 3 (on the right); i.e. a matrix that contains the volumes of traffic flowing between the nodes.

	NA	SA	BN	CE	FROM	NA	SA	BN	CE
NA	1	1	0	1	NA	0.7	0.1	0.1	0.1
SA	1	1	1	0	SA	0.8	0	0.1	0.1
BN	0	1	1	1	BN	0.8	0.1	0	0.1
CE	1	0	1	1	CE	0.8	0.1	0.1	0

Fig. 3. Example of RIMIC connectivity (left) and traffic (right) matrices for a particular hour of the day.

Each node is connected with itself in the connectivity matrix, as well as with the other nodes. This is to handle node disruption and traffic of links not considered in this simplified topology, but present in the full topology of the network, where secondary loops are attached to each node of the main loop.

The traffic matrix reported in the figure above is based on the following assumptions: (i) nodes have equal behavior in terms of traffic in input and output to/from them with the only exception of the node in Naples that is also the gateway to the internet and therefore all the traffic will pass through it; (ii) each node sends 0.1 traffic units (TUs) towards the others and 0.7 TUs towards the internet (through Naples-POP); (iii) each node sends and receives no traffic towards itself, except Naples (i.e., the one towards the internet).

The sum of the sum of values of the columns represents the total traffic (T_{tot}) delivered to destinations at a particular hour. After a seismic event, each link and node of the main loop is either considered still working or broken using the vulnerability models described above. Then, the performance of the network is evaluated: in details, a new connectivity matrix (C') is created from the original one (C), setting to 0 the values corresponding to links and nodes broken. The traffic matrix (T) is first scaled by the factor a to take into account the hour of day, then updated, multiplying each value of the new connectivity matrix times the corresponding value of the original, baseline traffic matrix. This is shown in Eq. (5) in which the generic element of the matrix at line s and column q is indicated by (s,q) :

$$T'(s,q) = C'(s,q) \cdot T(s,q) \quad (5)$$

The amount of total traffic that cannot be delivered is then computed and saved (i.e., traffic lost, T_{lost}). This metric has been chosen as PI for the case study; i.e.:

$$PI = T_{lost} = T_{tot} - T_{left} \quad (6)$$

where T_{left} corresponds to the sum of the sum of values of the columns of T' . It is worth noting that the current performance analysis considers the amount of traffic that is correctly transferred through the network before and after the event and uses the amount of traffic lost, calculated through a connectivity analysis, as a performance parameter. Doing this, it is implicitly assumed that all the links in the network are over-provisioned with respect to the traffic, so that, after the event, they are able to carry also the additional traffic rerouted through them because of the failure of some other link. This assumption is acceptable for the network under study because: (i) the links are all made of fiber optics with very high capacity (10/100Gpbs), and (ii) the number of users is still low because the network is relatively new. Moreover, it is also assumed that the failures can always be recovered through *physical-layer mechanisms* (as long as a fiber optics still exists between the nodes). In practice, there is no need to use the *IP-layer mechanisms*. This assumption has been verified for the network under study with the network designers, and it is true for the main backbone, that is the subject of the current paper.

6. Preliminary results

According to the flowchart of Fig. 4, thirty-thousands Monte Carlo simulations (i.e., thirty-thousands simulated earthquakes) were performed.

The annual rate of exceedance of the PI, $\lambda_{Traffic\ Lost}$, can be computed multiplying the cumulative rate of occurrence of the simulated earthquakes on the seismic sources (see Table 1),

with the probability of exceeding a predefined level of traffic lost; i.e., complementary cumulative distribution function of the chosen PI computed given to the occurrence of a generic earthquake (i.e., an earthquake of unknown magnitude and location).

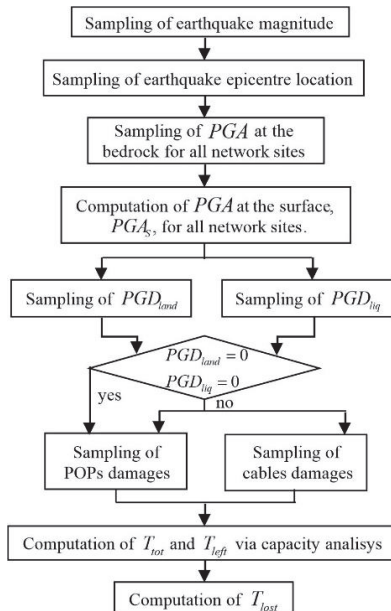


Fig. 4. Flowchart of a generic run of the Monte Carlo simulation.

Fig. 5 shows $\lambda_{Traffic\ Lost}$ as a function of T_{lost} computed in the two hypotheses of cables fragility. Given all the assumptions discussed, these preliminary results suggest a minor influence of cable fragilities.

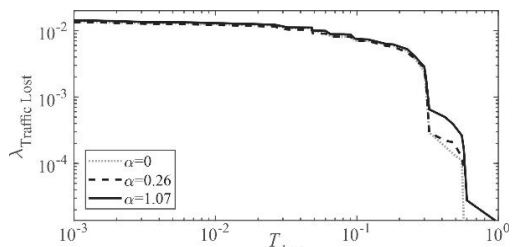


Fig. 5. Annual rate of exceedance of T_{lost} computed according to the three hypotheses on cables fragilities.

To stress this issue, the analysis was repeated assuming the α parameter of Eq. (4) equal to zero. The result is reported in the same figure. As shown, the influence of α is negligible for T_{lost} lower than about 0.3. Then a drop of $\lambda_{Traffic\ Lost}$ is observed and the vulnerability of the cables start having some effects.

7. Conclusions

In this study the probabilistic seismic risk assessment of a data communication network was discussed. The considered network is the main loop of the RIMIC network connecting the universities in the Campania region. The seismological, geological and geotechnical features of the region were characterized. Subsequently, the vulnerability of the physical assets of the network was modelled. In particular, due to the absence of specific fragility models, the empirical fragility functions developed for electrical buried cables are adopted herein. The performance of the network was quantified through the capacity of the network expressed in terms of total traffic delivered to each destination before and after the seismic event. The analyses were performed via Monte Carlo simulations.

Results, which must be considered very preliminary, are quantified in terms of annual rate of exceedance of the traffic lost, and suggest a low influence of the cables fragility on the network performance.

References

- Barani, S., D. Spallarossa, and P. Bazzurro (2009). Disaggregation of Probabilistic Ground Motion Hazard in Italy. *Bull. Seismol. Soc. Am.* 99 (5): 2638–61.
- Bommer, J.J., S. Akkar, and S. Drouet (2012). Extending Ground-Motion Prediction Equations for Spectral Accelerations to Higher Response Frequencies. *Bull. Earthq. Eng.* 10 (2): 379–99.
- Cavalieri, F., P. Franchin, and S. Buritica Cortes, J. A. M., Tesfamariam (2014). Models for Seismic Vulnerability Analysis of Power Networks: Comparative Assessment. *Comput. Civ. Infrastruct. Eng.* 29 (8): 590–607.
- Chang, L. and Z. Wu (2011). Performance and Reliability of Electrical Power Grids under Cascading Failures. *Int. J. Electr. Power Energy Syst.* 33 (8): 1410–19.
- Esposito, S., A. Botta, M. De Falco, I. Iervolino, A. Pescapè, and A. Santo (2018). Seismic Risk Analysis of Data Communication Networks: A Feasibility Study. In *16th Eur. Conf. Earthq. Eng.*, 1–12.
- Esposito, S. and I. Iervolino (2011). PGA and PGV Spatial Correlation Models Based on European Multievent Datasets. *Bull. Seismol. Soc. Am.* 101 (5): 2532–41.
- Esposito, S., I. Iervolino, A. Onofrio, A. Santo, F. Cavalieri, and P. Franchin (2015). Simulation-Based Seismic Risk Assessment of Gas Distribution Networks. *Comput. Civ. Infrastruct. Eng.* 30: 508–23. <https://doi.org/10.1111/mice.12105>.
- FEMA. 2004. *Multi-Hazard Loss Estimation Methodology: Earthquake Model: HAZUS MR4, Technical Manual*.
- Forte, G., S. Fabbrocino, G. Fabbrocino, G. Lanzano, Santucci de Magistris, and F. Silvestri (2017). A Geolithological Approach to Seismic Site Classification: An Application to the Molise Region (Italy). *Bull. Earthq. Eng.* 15 (1): 175–98.
- Franchin, P. and F. Cavalieri (2013). *Seismic Vulnerability Analysis of a Complex Interconnected Civil Infrastructure*. <https://doi.org/10.1533/9780857098986.4.465>.
- Gutenberg, R., and C.F. Richter (1944). Frequency of Earthquakes in California. *Bull. Seismol. Soc. Am.* 34: 185–88.
- Jayaram, N., and J.W. Baker (2009). Correlation Model for Spatially Distributed Ground Motion Intensities. *Earthq. Eng. Struct. Dyn.* 38 (15): 1687–708.
- Kongar, I., S. Giovinazzi, and T. Rossett. (2017). Seismic Performance of Buried Electrical Cables: Evidence-Based Repair Rates and Fragility Functions. *Bull. Earthq. Eng.* 15 (7): 3151–81.
- Liao, S.S.C., D. Veneziano, and R.V. Whitman (1988). Regression Models for Evaluating Liquefaction Probability. *J. Geotech. Eng.* 114 (4): 389–411.
- Loth, C., and J.W. Baker (2013). A Spatial Cross-Correlation Model of Spectral Accelerations at Multiple Periods. *Earthq. Eng. Struct. Dyn.* 42 (June): 397–417. <https://doi.org/10.1002/eqe>.
- Meletti, C., F. Galadini, G. Valensise, M. Stucchi, R. Basili, S. Barba, G. Vannucci, and E. Boschi. (2008). A Seismic Source Zone Model for the Seismic Hazard Assessment of the Italian Territory. *Tectonophysics* 450: 85–108.
- Petruzzelli, F. and I. Iervolino. 2014. FRAME V.1.0: A Rapid Fragility-Based Seismic Risk Assessment Tool. In *Second Eur. Conf. Earthq. Eng. Seismol. 2ECEES, – Istanbul, Turkey, August 24-29*.
- Saygili, G. and E.M. Rathje (2008). Empirical Predictive Models for Earthquake-Induced Sliding Displacements of Slopes. *J. Geotech. Geoenvironmental Eng.* 134 (6): 790–803.
- Seed, H.B. and I.M. Idriss (1982). Ground Motions and Soil Liquefaction During Earthquakes. Oakland, California.
- Tokimatsu, K. and H.B. Seed (1987). Evaluation of Settlement in Sands Due to Earthquake Shaking. *J. Geotech. Geoenvironmental Eng.* 113 (8): 861–878.
- Vanzi, I. (1996). Seismic Reliability of Electric Power Networks: Methodology and Application. *Struct. Saf.* 18 (4): 311–27.
- Weatherill, G., S. Esposito, I. Iervolino, P. Franchin, and F. Cavalieri (2014). Framework for Seismic Hazard Analysis of Spatially Distributed Systems. *Geotech. Geol. Earthq. Eng.* 31: 57–88.
- Wilson, R.C., and D.K. Keefer (1985). Predicting Areal Limits of Earthquake Induced Landsliding. In *Eval. Earthq. Hazards Los Angeles Reg. U.S. Geol. Surv. Prof. Pap.*, edited by J. I. Ziony, 317–45.